Sparse Target Localization in RF Sensor Networks using Compressed Sensing

Heping Song[1], Guoli Wang[2], Yongzhao Zhan[1]

1. School of Computer Science and Telecommunication Engineering, Jiangsu University, Zhenjiang, Jiangsu 212013, China

2. School of Information Science and Technology, Sun Yat-Sen University, Guangzhou, Guangdong 510006, China

E-mail: songhp@ujs.edu.cn

Abstract: In this paper, we propose a greedy sparse recovery algorithm for target localization with RF sensor networks. The target spatial domain is discretized by grid pixels. When the network area consists only of several targets, the target localization is a sparsity-seeking problem such that the Compressed Sensing (CS) framework can be applied. We cast the target localization as a CS problem and solve it by the proposed sparse recovery algorithm, named the Residual Minimization Pursuit (RMP). The experimental studies are presented to demonstrate that the RMP offers an attractive alternative to OMP for sparse signal recovery, in addition, it is more favorable than non-CS based methods for target localization.

Key Words: Target Localization, Sparse Recovery, Compressed Sensing, RF Sensor Networks

1 INTRODUCTION

Device-free passive localization (DFL) in wireless sensor networks (WSN) is a cost-effective technique for inferring the locations of targets [1]. Compared with active localization techniques such as global positioning system (GPS), radio frequency identification (RFID) and real-time location system (RTLS), the DFL does not require the targets to carry devices. A number of possible sensor technologies including optical cameras, thermal cameras, passive infrared, acoustic, vibration and ultrasound, could be used for the purposes of DFL. Radio frequency (RF) signals can travel through opaque obstructions without privacy concerns, such as nonmetal walls, trees, and smoke while optical or infrared sensors cannot. Using received signal strength (RSS) measurements in RF based DFL is preferable to many WSN applications.

Recently, Wilson and Patwari developed a new technology for DFL, referred to radio tomographic imaging (RTI) [2, 3]. The scene of interest is imaged from attenuation caused by targets present in wireless network area. RTI obtains current images of the locations of targets. RTI explores a linear model which relates the attenuation field to signal strength measurements. The least-squares solution for the linear formulation is an ill-posed inverse problem by nature. However, RTI does not indicate the actual locations of targets due to lack of contrast needed to accurately distinguish the locations. It does not make use of the sparse nature of location finding problem. Hence we propose a new approach by exploiting the sparse recovery power of Compressed Sensing (CS).

CS is an emerging technique that provides a framework for sparse recovery [4, 5], which indicates that sparse or compressible signals can be recovered from far fewer samples. CS was originally proposed in the signal processing community [4, 5], and has been applied to WSN applications in [6, 7]. The sparse nature of the location finding problem makes the theory of CS desirable for target localization in RF sensor networks. Inspired by success of [6, 7], we cast the RTI formulation as a sparse recovery problem and present an efficient algorithm. The proposed algorithm is called Residual Minimization Pursuit (RMP). In our method, as opposed to least-squares type methods used in [2, 3], we directly determine where the targets located in the network area.

The rest of the paper is organized as follows. The problem formulation and the proposed approach are presented in section 2. After that, section 3 details the experimental results on simulated data and real data. Finally, we conclude this paper in section 4.

Notation

We introduce the notation used in this paper:

- x_t: the algorithms described in this paper are iterative and the reconstructed signal x in current iteration t is denoted as x_t. The same convention is used for other vectors and matrices.
- I, A_I: index set I, the matrix A_I denotes the submatrix of A containing only those columns of A with indexes in I. The same convention is used for vectors.
- $[1, n] \backslash I$: the complement of set I in set $\{1, 2, \cdots, n\}$.
- $\mathrm{supp}(x)$: the support set of a vector x, i.e. the index

Special thanks to Bob Sturm, who provided the code for phase transitions, and Joey Wilson & Neal Patwari, who shared the RTI dataset. This work was supported by the National Science Foundation of China under Grant no. 61074167, 61170126, 61202110 and the Scientific Research Foundation for Advanced Talents by the Jiangsu University, no. 12JDG050.

978-1-4673-5534-6/13/$31.00

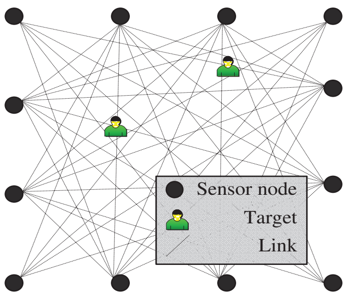

Figure 1: A twelve RF nodes wireless sensor network. Each wireless RF node communicates with the others.

set corresponding to the nonzeros of x, $\text{supp}(x) = \{i : x_i \neq 0\}$.

- $|x|$, $\|x\|_p$, x^T: the absolute value, ℓ_p norm and transpose of a vector x, respectively.
- $A^\dagger$: the Moore-Penrose pseudoinverse of matrix $A \in \mathbb{R}^{m\times n}$. $A^\dagger = A^T(AA^T)^{-1}$ for $m \leq n$; $A^\dagger = (A^TA)^{-1}A^T$ for $m \geq n$.

2 METHOD

2.1 Problem Formulation

Consider a RF sensor network, as illustrated in Figure 1, the RF signal is affected by the presence of the targets near the wireless links. We can infer the locations of attenuating targets from pairwise RSS measurements which caused by shadowing correlations between links. As shown in Figure 2, the network area is divided into grid pixels $\mathrm{x} \in \mathbb{R}^n$. The amount of radio power attenuation describes each pixel's value. The attenuation of unique two-way links (the communication between any pair of distinguishable nodes.) can be denoted as $\mathrm{y} \in \mathbb{R}^m$. This can be formulated as a linear model, take the form of

$$\mathrm{y} = A\mathrm{x} + \mathrm{n}. \tag{1}$$

The link shadowing is a linear combination of the values in pixels, plus noise n. $\mathrm{y} \in \mathbb{R}^m$ is the difference of RSS measurements that the instantaneous RSS value vector subtracts the average background RSS value vector. $A \in \mathbb{R}^{m\times n}$ is the weight matrix of the model parameter x. Each row of the weight matrix on the link i can be expressed a weighted sum of the losses in each pixel. The weight matrix A for link shadowing can be described by an ellipsoid with foci at each pair of nodes locations [2, 3], as shown in Figure 3. d is the link distance between the nodes, $d_{ij}(1)$ and $d_{ij}(2)$ are the distance from pixel j to the two nodes for link i. If a pixel falls inside the ellipse, it is weighted and normalized by square root of the link distance, otherwise, the weight is set to zero. The elliptical width parameter λ is a tradeoff between modeling error and tracking performance. For the most accurate localization, we set to 0.01 in our experiments.

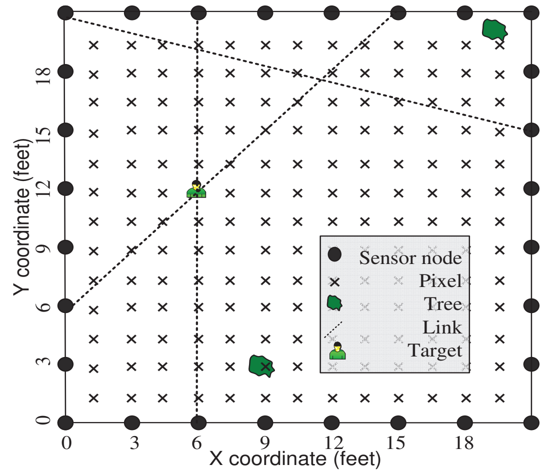

Figure 2: The network geometry with one target locating at (6, 12). The tracked area is divided in to 13×13 pixels.

2.2 The Proposed Algorithm

When positioning targets from RSS measurements, it is an inverse problem from (1) to get the pixels attenuation x. x can determine where the targets are located in the network area. Generally, it formulates the inverse problem in the least-squares error sense [2, 3],

$$\mathrm{x}_{LS} = \arg\min ||A\mathrm{x} - \mathrm{y}||_2^2. \tag{2}$$

Regularization methods were introduced into the linear model to alleviate the singularity problem and make the inverse problem stable [2, 3]. All least-squares solutions minimize the noise energy, and the results are very smooth. It must have a contrast step to estimate the locations of targets. Thus RTI does not indicate the actual locations of targets. We cast the inverse problem (1) as a compressed sensing problem motivated by the sparse nature of location finding problem. Sparse recovery algorithms for CS problem have two major classes, greedy algorithms and ℓ_1 norm minimization. ℓ_1 norm minimization algorithms (e.g. Basis Pursuit [8]) are not feasible solutions due to high computational complexity and instability rises in measurements noise. In this paper, we consider the greedy algorithms for target localization. Greedy sparse recovery algorithms, e.g. orthogonal matching pursuit (OMP) [9], iterate between 2 main steps:

1. **Support detection:** the algorithms detect the support set of the signal x, i.e. select atoms of measurement matrix A which have been used to generate y in other words, determine active atoms in sparse representation of a signal x. In some literatures, this step also is called basis selection or atom selection.
2. **Signal estimation:** update the signal using the least-squares solution on the detected support set.

Recently, Yang et al. proposed a new sparse recovery algorithm, referred to orthogonal pruning pursuit (OPP) [10]. OPP derives a heuristic criterion from preserving a minimum residual by pruning a redundant basis successively. It

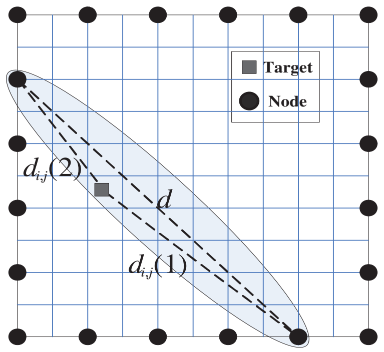

Figure 3: Elliptical weight model, the weighted pixels for a single link in a RF sensor network are darkened in an ellipse with foci at each node location.

can be seen that the support detection strategy minimizes the increase of the residual norm at each iteration. OPP shrinks the support set I by pruning a basis A_j , the criterion is given by

$$\arg\min_{j} \frac{(\hat{\mathrm{x}}_j)^2}{||A_j||_2^2}. \tag{3}$$

where $\hat{\mathrm{x}}$ is the least-squares solution on support set I (i.e. $\hat{\mathrm{x}} = A_I^{\dagger}\mathrm{y}$). A_j is the column of corresponding index j. Motivated by OPP, we present a dual criterion, which is given by

$$\arg\max_{j} \frac{(\{A^{\dagger}\mathrm{r}\}_j)^2}{||A_j||_2^2}, \mathrm{r} = \mathrm{y} - A\mathrm{x}_{t-1}. \tag{4}$$

where $A^{\dagger} = A^T(AA^T)^{-1}$ is the Moore-Penrose pseudoinverse of the measurement matrix A. t denotes the iteration index. r is the residual signal. We assume the columns of the measurement matrix A are scaled to unit L_2 norm for convenience (i.e. $||A_j||_2 = 1$). We present a new algorithm, termed as residual minimization pursuit (RMP). The detailed description (given in Algorithm 1) of the proposed algorithm is presented as follows

Step 1: Initialization:
Initialize the residual signal $\mathrm{r}_0 = \mathrm{y}$,
initialize the support set $I_0 = \emptyset$,
and set the iteration counter $t = 1$.

Step 2: Support detection:
Find the index j that maximize the magnitude of $A^{\dagger}\mathrm{r}_{t-1}$,
and augment the support set $I_t = I_{t-1} \cup \{j\}$.

Step 3: Signal estimation:
Estimate the signal:
$\mathrm{x}_{I_t} = A_{I_t}^{\dagger}\mathrm{y}$,
$\mathrm{x}_{[1,n]\setminus I_t} = 0$,
$\mathrm{r}_t = \mathrm{y} - A\mathrm{x}_t$.

Step 4: Halting:
Increment t and return to Step 2 if $t < k$ (k is the true underlying sparsity level of signal x), otherwise the algorithm is terminated. The recovered signal x has nonzero entries in support set I_t and the corresponding support vector lies in x_{I_t}.

Algorithm 1 Residual Minimization Pursuit

Input: Measurement matrix A, measurements y, sparsity level k
Output: The reconstructed signal x

```
Initialization:
  t  = 1 //iteration number
  r_0  = y //initial residual
  I_0  = ∅ //initial support set
for t = 1 : k do
  I_t = I_{t-1} ∪ { index of the largest entry of |A^† r_{t-1}| }
  x_{I_t} = A^†_{I_t} y
  x_{[1,n]\I_t} = 0
  r_t = y − A x_t
end for
return x
```

Remarks:

1. OMP uses the correlation between the residual signal and the atoms of the measurement matrix A to select one active atom at each iteration. The support detection strategy is correlation maximization while RMP is residual minimization.

2. RMP is identical to OMP when the measurement matrix A has orthonormal rows (that is (AA^T) is the identity matrix). RMP is the dual formulation of OPP by maximizing decrease of the residual norm.

3. RMP and OMP forward select one active nonzero entry at a time (i.e. k iterations), while OPP backward deselects one inactive zero entry at a time (i.e. $n-k$ iterations). RMP and OMP clearly converge in far fewer iterations than OPP ($k \ll n - k$).

3 EXPERIMENTAL RESULTS

To assess the performance of the proposed approach, we conduct experiments on computer simulations and real RTI dataset.

3.1 Computer Simulations

We assess the sparse recovery performance in terms of phase transitions [11, 12]. Let $\rho = k/m$ be a normalized measure of the sparsity and let $\delta = m/n$ be a normalized measure of problem indeterminacy. We obtain a two dimensional phase space $(\delta, \rho) \in [0, 1]^2$ measuring the sparse recovery performance. The phase space is divided into two regions by a curve. The lower right region indicates the success of sparse recovery. The curve dubbed as phase transition curve. Detailed definition of the phase transition curve is described in [11, 12]. A higher phase transition curve indicates better sparse recovery performance. The problem suit (A, x) is nearly similar to [11, 13]. Let A be a random matrix with i.i.d. Gaussian entries and each column be normalized with unit norm. We fixed $n = 400$, sampled 16 different linearly spaced sparsity $\rho \in [0.05, 0.5]$ and indeterminacies $\delta \in [0.05, 0.5]$. We take 100 times

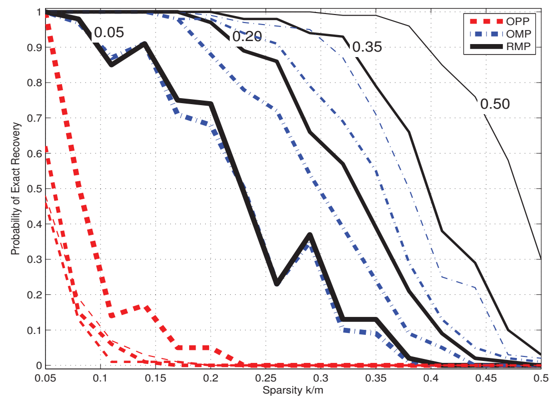

Figure 4: Recovery rates of OPP, OMP and RMP for 4 different indeterminacies (m/n, labeled) and sparse vector distributed Gaussian.

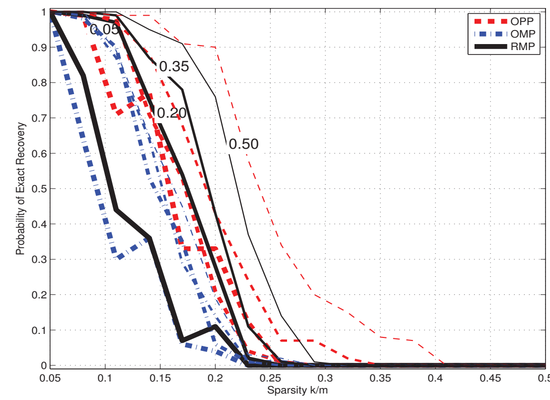

Figure 6: Recovery rates of OPP, OMP and RMP for 4 different indeterminacies (m/n, labeled) and sparse vector distributed Bernoulli.

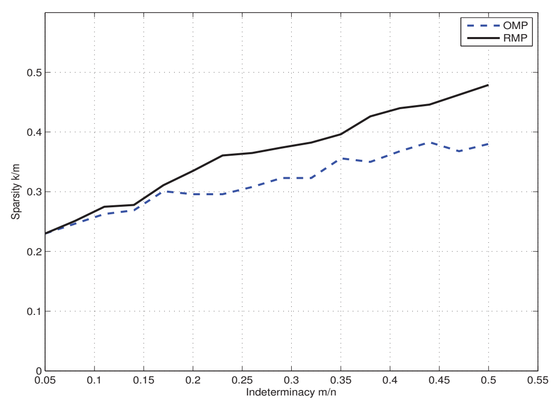

Figure 5: Phase transitions of OMP and RMP for sparse vector distributed Gaussian.

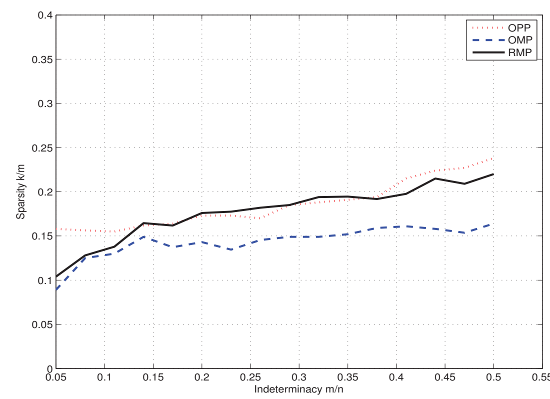

Figure 7: Phase transitions of OPP, OMP and RMP for sparse vector distributed Bernoulli.

Monte Carlo problem instances and declare exact recovery if $\|\mathrm{x} - \hat{\mathrm{x}}\|_2/\|\mathrm{x}\|_2 < 0.01$. According to the observation of [13, 14], greedy methods exhibit superior performance for sparse vector distributed Gaussian and inferior performance for sparse vector distributed Bernoulli. We generate k sparse vector distributed Gaussian and Bernoulli. Figure 4 and Figure 5 present the recovery performance of OPP, OMP and RMP for sparse vector distributed Gaussian. We omit the phase transition curve of OPP here due to high complexity of plot. It shows that RMP outperforms OPP and OMP. For sparse vector distributed Bernoulli, Figure 6 and Figure 7 show the recovery performance of OPP, OMP and RMP. OPP performs better than RMP and OMP. However, RMP appears more robust than OPP and OMP to distribution underlying sparse vector.

3.2 Target Localization Application

To validate the effectiveness of the proposed method, the experiments were conducted on a real outdoor environment using an IEEE 802.15.4 (Zigbee) protocol in the 2.4GHz fre-quency band network. The RTI dataset [3] is available online at http://span.ece.utah.edu/rti-data-set. A 28 nodes peer-to-peer network was deployed in a square perimeter of 21 feet $\times$ 21 feet and each side has 8 nodes, as depicted in Figure 2. Each node was spaced 3 feet from the neighboring nodes. Two trees surround the border of the network with approximately 1 foot diameter trunks. The difference of RSS measurements was obtained by the instantaneous RSS value vector subtracting the average background RSS value vector. Each link's measurement is an average of the two directional links from i to j and j to i. The background RSS value vector was measured when the network area was vacant from targets. We create grid pixels x within the network area using resolution 6×6, 13×13 and 27×27. To quantify the accuracy of localization, we employ average error, which is defined as follow

$$e = \frac{1}{k}\sum_{i=1}^{k}\sqrt{(\mathrm{x}_i - \hat{\mathrm{x}}_i)^2 + (\mathrm{y}_i - \hat{\mathrm{y}}_i)^2}, \quad (5)$$

where k is the number of targets, $< \mathrm{x}_i, \mathrm{y}_i >$ is the actual coordinate and $< \hat{\mathrm{x}}_i, \hat{\mathrm{y}}_i >$ is the estimated location. Figure 8 - 13 present the results with two targets located at coordinate (3, 15) and (15, 15) respectively. RTI results do not indicate the actual locations of targets, However, RMP ex-

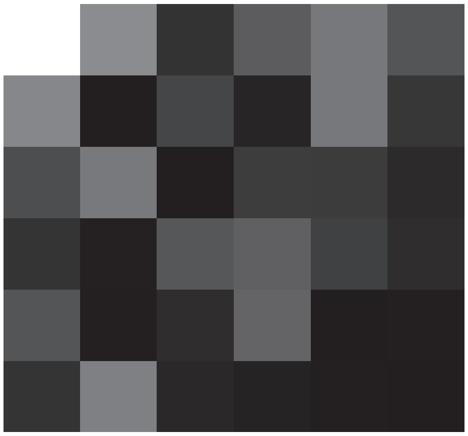

Figure 8: RTI result using resolution 6 × 6.

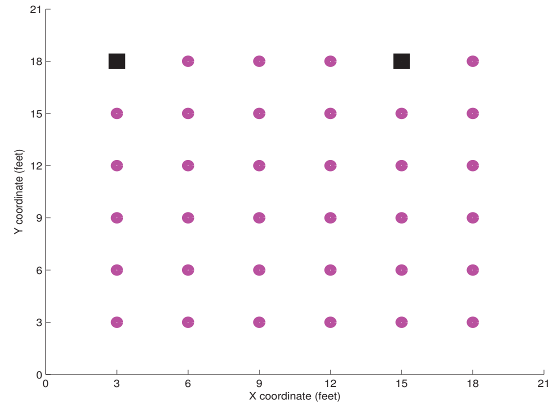

Figure 9: Estimated locations using RMP with resolution 6 × 6. The magenta circle is the pixel and the black square is the location of target.

hibits reliable locations. RMP can be viewed as a contrast step to estimate the locations of targets. The average errors are 2.12 feet, 1.68 feet and 1.45 feet using resolution 6 × 6, 13 × 13 and 27 × 27 respectively. Target localization using higher resolution obtains better performance and higher precision level.

4 CONCLUSIONS

In this paper, we propose a novel target localization algorithm based on the emerging compressed sensing (CS) signal recovery paradigm for WSN applications. Motivated by the sparse nature of location finding problem, we cast target localization as a sparse recovery problem and solve it by the proposed Residual Minimization Pursuit (RMP) algorithm. We investigate the effectiveness of the proposed algorithm on computer simulations and real localization application. The experimental results demonstrate that RMP offers an attractive alternative to OMP for signal recovery, and RMP is more favorable than non-CS based methods for target localization.

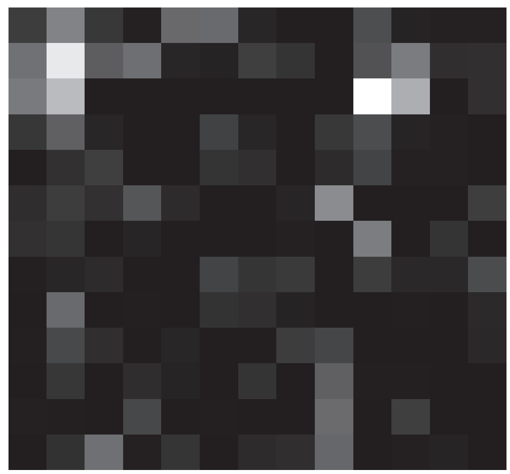

Figure 10: RTI result using resolution 13 × 13.

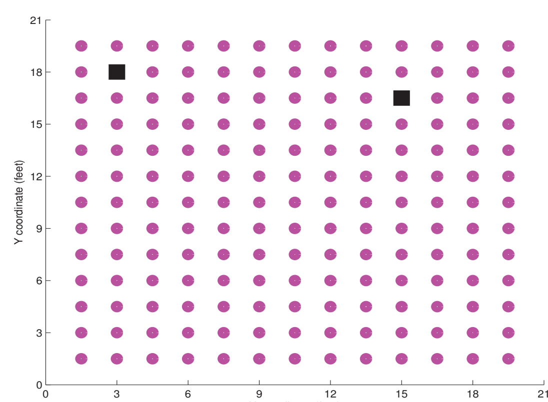

Figure 11: Estimated locations using RMP with resolution 13 × 13. The magenta circle is the pixel and the black square is the location of target.

REFERENCES

[1] M. Youssef, M. Mah, and A. Agrawala, "Challenges: Device-free passive localization for wireless environments," in *Proceedings of the 13th annual ACM international conference on Mobile computing and networking*. New York, NY, USA: ACM, 2007, pp. 222–229.

[2] N. Patwari and P. Agrawal, "Effects of correlated shadowing: connectivity, localization, and rf tomography," in *ACM/IEEE International Conference on Information Processing in Sensor Networks*. St. Louis, Missouri, USA: IEEE, April 22-24 2008, pp. 82–93.

[3] J. Wilson and N. Patwari, "Radio tomographic imaging with wireless networks," *IEEE Transactions On Mobile Computing*, vol. 9, no. 5, pp. 621–632, 2010.

[4] E. Candes, J. Romberg, and T. Tao, "Robust uncertainty principles: Exact signal reconstruction from highly incomplete frequency information," *IEEE Transactions on Information Theory*, vol. 52, no. 2, pp. 489–509, 2006.

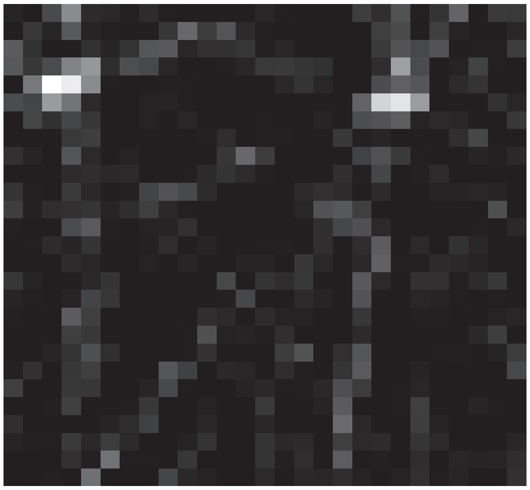

Figure 12: RTI result using resolution 27 × 27.

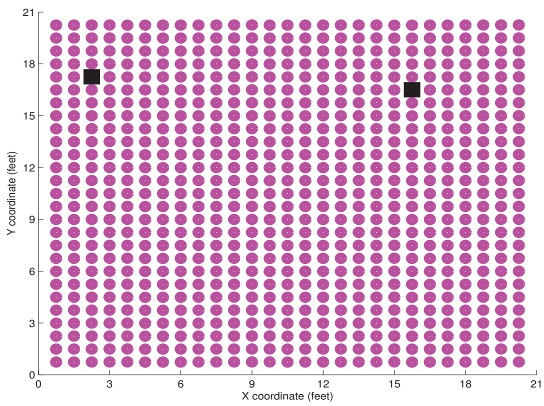

Figure 13: Estimated locations using RMP with resolution 27 × 27. The magenta circle is the pixel and the black square is the location of target.

[5] D. Donoho, "Compressed sensing," *IEEE Transactions on Information Theory*, vol. 52, no. 4, pp. 1289–1306, 2006.

[6] C. Feng, S. Valaee, and Z. Tan, "Multiple target localization using compressive sensing," in *IEEE Global Telecommunications Conference*, Honolulu, HI, Nov. 30 - Dec. 4 2009, pp. 1–6.

[7] J. Meng, H. Li, and Z. Han, "Sparse event detection in wireless sensor networks using compressive sensing," in *Annual Conference on Information Sciences and Systems*, Baltimore, MD, March 18-20 2009, pp. 181–185.

[8] D. Chen, S.and Donoho and M. Saunders, "Atomic decomposition by basis pursuit," *SIAM Review*, vol. 43, no. 1, pp. 129–159, 2001.

[9] J. Tropp and A. Gilbert, "Signal recovery from random measurements via orthogonal matching pursuit," *IEEE Transactions on Information Theory*, vol. 53, no. 12, pp. 4655–4666, 2007.

[10] D. Yang, H. Li, and G. Peterson, "Feedback orthogonal pruning pursuit for pulse acquisition in uwb communications," in *IEEE 20th International Symposium on Personal, Indoor and Mobile Radio Communications*, Tokyo, Japan, Sept. 13-16 2009, pp. 1647–1651.

[11] A. Maleki and D. Donoho, "Optimally tuned iterative reconstruction algorithms for compressed sensing," *IEEE Journal of Selected Topics in Signal Processing*, vol. 4, no. 2, pp. 330–341, 2010.

[12] D. Donoho and J. Tanner, "Precise undersampling theorems," *Proceedings of the IEEE*, vol. 98, no. 6, pp. 913–924, june 2010.

[13] B. Sturm, "A study on sparse vector distributions and recovery from compressed sensing," *arxiv:1103.6246*, 2011.

[14] X. Zhang, J. Wen, Y. Han, and J. Villasenor, "An improved compressive sensing reconstruction algorithm using linear non-linear mapping," in *Information Theory and Applications Workshop*, UC San Diego, USA, Feb. 6 - 11, 2011, pp. 1–7.